

## **Estimating Movement Rates Between Eurasian and North American Birds That Are Vectors of Avian Influenza**

Authors: Spaulding, Fern, McLaughlin, Jessica F., Glenn, Travis C., and Winker, Kevin

Source: Avian Diseases, 66(2) : 1-10

Published By: American Association of Avian Pathologists

URL: <https://doi.org/10.1637/aviandiseases-D-21-00088>

---

BioOne Complete ([complete.BioOne.org](https://complete.BioOne.org)) is a full-text database of 200 subscribed and open-access titles in the biological, ecological, and environmental sciences published by nonprofit societies, associations, museums, institutions, and presses.

Your use of this PDF, the BioOne Complete website, and all posted and associated content indicates your acceptance of BioOne's Terms of Use, available at [www.bioone.org/terms-of-use](https://www.bioone.org/terms-of-use).

Usage of BioOne Complete content is strictly limited to personal, educational, and non-commercial use. Commercial inquiries or rights and permissions requests should be directed to the individual publisher as copyright holder.

---

BioOne sees sustainable scholarly publishing as an inherently collaborative enterprise connecting authors, nonprofit publishers, academic institutions, research libraries, and research funders in the common goal of maximizing access to critical research.

## Original Article—

## Estimating Movement Rates Between Eurasian and North American Birds That Are Vectors of Avian Influenza

Fern Spaulding,<sup>ABE</sup> Jessica F. McLaughlin,<sup>C</sup> Travis C. Glenn,<sup>D</sup> and Kevin Winker<sup>AB</sup>

<sup>A</sup>University of Alaska Museum, University of Alaska Fairbanks, Fairbanks, AK 99775

<sup>B</sup>Department of Biology and Wildlife, University of Alaska Fairbanks, Fairbanks, AK 99775

<sup>C</sup>Department of Environmental Science, Policy, and Management, University of California Berkeley, Berkeley, CA 94720

<sup>D</sup>Department of Environmental Health Science and Institute of Bioinformatics, University of Georgia, Athens, GA 30602

Received 17 September 2021; Accepted 9 December 2021; Published ahead of print 2 May 2022

**SUMMARY.** Avian influenza (AI) is a zoonotic disease that will likely be involved in future pandemics. Because waterbird movements are difficult to quantify, determining the host-specific risk of Eurasian-origin AI movements into North America is challenging. We estimated relative rates of movements, based on long-term evolutionary averages of gene flow, between Eurasian and North American waterbird populations to obtain bidirectional baseline rates of the intercontinental movements of these AI hosts. We used population genomics and coalescent-based demographic models to obtain these gene-flow-based movement estimates. Inferred rates of movement between these continental populations varies greatly among species. Within dabbling ducks, gene flow, relative to effective population size, varies from ~3 to 24 individuals/generation between Eurasian and American wigeons (*Mareca penelope* and *Mareca americana*) to ~100–300 individuals/generation between continental populations of northern pintails (*Anas acuta*). These are evolutionary long-term averages and provide a solid foundation for understanding the relative risks of each of these host species in potential intercontinental AI movements. We scale these values to census size for evaluation in that context. In addition to being AI hosts, many of these bird species are also important in the subsistence diets of Alaskans, increasing the risk of direct bird-to-human exposure to Eurasian-origin AI virus. We contrast species-specific rates of intercontinental movements with the importance of each species in Alaskan diets to understand the relative risk of these taxa to humans. Assuming roughly equivalent AI infection rates among ducks, greater scaup (*Aythya marila*), mallard (*Anas platyrhynchos*), and northern pintail (*Anas acuta*) were the top three species presenting the highest risks for intercontinental AI movement both within the natural system and through exposure to subsistence hunters. Improved data on AI infection rates in this region could further refine these relative risk assessments. These directly comparable, species-based intercontinental movement rates and relative risk rankings should help in modeling, monitoring, and mitigating the impacts of intercontinental host and AI movements.

**RESUMEN.** Estimación de las tasas de movimiento entre aves euroasiáticas y norteamericanas que son vectores de la influenza aviar.

La influenza aviar es una enfermedad zoonótica que probablemente estará involucrada en futuras pandemias. Debido a que los movimientos de aves acuáticas son difíciles de cuantificar, la determinación del riesgo específico de hospedador de los movimientos de influenza aviar de origen euroasiático en América del Norte es un desafío. Se estimaron las tasas relativas de movimientos, sobre la base de promedios evolutivos a largo plazo del flujo de genes, entre las poblaciones de aves acuáticas euroasiáticas y norteamericanas para obtener tasas de referencia bidireccionales de los movimientos intercontinentales de estos huéspedes de influenza aviar. Se utilizó genómica de poblaciones y modelos demográficos basados en la teoría de la coalescencia para obtener estas estimaciones de movimiento basadas en el flujo de genes. Las tasas inferidas de movimiento entre estas poblaciones continentales varían mucho entre especies. Dentro de los patos chapuceros, el flujo de genes, en relación con el tamaño efectivo de la población, varía aproximadamente de 3 a 24 individuos/generación entre los silbones europeos y americanos (*Mareca penelope* y *Mareca americana*) hasta aproximadamente entre 100 a 300 individuos/generación entre poblaciones continentales de ánades rabudos (*Anas acuta*). Estos son promedios evolutivos a largo plazo y proporcionan una base sólida para comprender los riesgos relativos de cada una de estas especies hospedadoras en posibles movimientos intercontinentales de la influenza aviar. Se evaluaron estos valores al tamaño del censo para evaluarlos en ese contexto. Además de ser huéspedes de influenza aviar, muchas de estas especies de aves también son importantes en las dietas de subsistencia de los habitantes de Alaska, lo que aumenta el riesgo de exposición directa de las aves al ser humano por el virus de la influenza aviar de origen euroasiático. Se contrastaron las tasas específicas de especies de movimientos intercontinentales con la importancia de cada especie en las dietas de personas en Alaska para comprender el riesgo relativo de estos taxones para los humanos. Suponiendo tasas de infección por influenza aviar aproximadamente equivalentes entre patos, el porrón bastardo o pato boludo mayor (*Aythya marila*), el ánade real (*Anas platyrhynchos*) y el ánade rabudo eran las tres especies principales que presentaban los mayores riesgos para el movimiento de influenza aviar intercontinental tanto dentro del sistema natural como a través de la exposición a cazadores de subsistencia. La mejora de los datos sobre las tasas de infección por influenza aviar en esta región podría mejorar aún más estas evaluaciones de riesgo relativo. Estas tasas de movimiento intercontinental directamente comparables, basadas en especies, y clasificaciones de riesgo relativo deberían ayudar a modelar, monitorear y mitigar los impactos de los movimientos intercontinentales de huéspedes y de la influenza aviar.

Key words: avian influenza, Beringia, waterfowl, gene flow, subsistence harvest, vector species, Alaska

Abbreviations: AI = avian influenza; AIC = Akaike information criterion; HPAI = highly pathogenic avian influenza;  $N_e$  = effective population size; SNP = single-nucleotide polymorphism; UCEs = ultraconserved elements; VCF = Variant Call Format

<sup>E</sup>Corresponding author. E-mail: Fern Spaulding; frspaulding@alaska.edu



Fig. 1. Beringia encompasses the region extending from the Russian Far East across the Bering Sea through Alaska to western Canada in North America. Across Beringia, waterbirds are important avian influenza (AI) vectors and are a staple in the rural subsistence diet.

## INTRODUCTION

Avian influenza (AI) is a zoonotic disease and will likely be involved in future pandemics (1,2,3,4). AI research and surveillance has demonstrated the exchange of viruses between Eurasia and North America through migratory birds that occur across the Beringian region, the area between Alaska and the Russian Far East (5,6,7,8,9,10). Beringia (Fig. 1) encompasses a large geographic area, and many birds migrate seasonally here to breed. Aquatic birds, such as waterfowl and shorebirds, are often asymptomatic carriers of the disease, indicating that they are well adapted to this pathogen and serve as a natural reservoir (11,12,13). Winker and Gibson (14) estimated that ~1.5–2.9 million birds that are likely vector species of AI virus migrate from Eurasia across Beringia to their breeding grounds in Alaska every year. This large overlap of Eurasian and North American migration systems causes extensive seasonal contact between these lineages and populations, resulting in a potential for virus movements into and out of North America (15,16). This vast number of seasonal migrants is often underappreciated when modeling AI introduction into North America (1,14,15,17,18,19,20,21). International borders and vast areas of remote land make accurate estimates of intercontinental AI host movements difficult. Yet knowing the degree of these movements between Eurasia and North America is critical to understanding intercontinental transmission of AI viruses.

In addition to being potential vectors of intercontinental virus transport, many of these waterfowl and shorebird species are a common staple in the subsistence diets of many Alaskans. Waterfowl in particular account for a large proportion of the annual wild bird harvest, making up approximately 85% of migratory birds taken for subsistence in Alaska (22). In Alaska, this annual bird subsistence harvest is approximately 20 times larger than annual commercial poultry production (23,24). These wild-bird interactions, then, are likely the predominant source of human-bird contacts in the state. Southward autumn migration of North American waterbird populations then enables AI virus transport that poses additional risk not only to hunters but also through spillover into domestic

poultry in regions where this form of agriculture is more common (25).

Influenza virus surveillance in Alaskan waterfowl has thus far found predominantly low pathogenic avian influenza (6,26,27). But lineages of highly pathogenic avian influenza (HPAI) of Eurasian origin have been detected in Alaskan populations (e.g., H9N2) (28). AI viral dispersal and transmission across Beringia is not a rare occurrence (7), and multiple examples of intercontinental exchange have been documented (5,7,13,28,29,30). Human contact with wild populations of waterfowl during hunting might cause AI exposure, a possibility supported by the detection of antibodies in humans to influenza virus subtypes (i.e., H11) found only in wild birds (31). Hunters will often process harvested birds themselves while in the field without using gloves or personal protective equipment (32). By processing an influenza-infected duck, a hunter might be exposed to virus-laden mucosa and excretions (i.e., nasal or fecal) in addition to blood, tissues, and other body fluids (32,33,34). Because waterfowl are an important subsistence food for Alaskans, contact while handling and processing these birds is a potential risk factor for direct bird-to-human transmission (35,36,37).

In this study, we used population genomics, using ultraconserved elements (UCEs) as a sequenced subsampling of the genome to improve rough estimates (14) of intercontinental AI host movements among key waterbird species to better understand the natural host-virus movement-transmission landscape in Beringia. Given Alaska's proximity to Eurasia, we also contrast these estimates with the importance of each species in Alaskan diets to understand the relative risk of these taxa directly to human consumers. This information can enable subsistence hunters to selectively harvest species that have a lower potential risk of carrying Eurasian-origin HPAI, or to process different species using different levels of personal protection. These relative risk rankings should help in modeling, monitoring, and mitigating the impacts of intercontinental host and AI movements.

## MATERIALS AND METHODS

**Sampling and laboratory.** Our samples consist of high-quality, vouchered tissue samples from wild birds of Eurasian and North American origin (Supplemental Table S1). Our study design includes pairwise comparisons of populations, subspecies, and species, because taxonomy is not a reliable indicator of intercontinental levels of gene flow (38,39,40). We chose birds based on sample availability for species commonly taken by subsistence hunters in Alaska. We sampled the following numbers of individuals for each vector species: 10 northern pintail (*Anas acuta*), 12 mallard (*Anas platyrhynchos*), 10 greater scaup (*Aythya marila*), 10 common eider (*Somateria mollissima*), and 9 common and Wilson's snipe (*Gallinago gallinago* and *Gallinago delicata*). We also incorporated the gene flow rates obtained by McLaughlin *et al.* (40), which include: green-winged teal (*Anas crecca crecca* and *A. c. carolinensis*), long-tailed duck (*Clangula hyemalis*), and Eurasian and American wigeons (*Mareca penelope* and *Mareca americana*). Using UCEs as a sequence-based subsampling of the genome allows us to examine thousands of orthologous loci (41), and it has been shown that, in general, relatively small sample sizes are sufficient when using coalescent methods to estimating population demographics (42,43,44). Here, we are particularly interested in levels of gene flow ( $m$ ), which when using our methods of analysis appear to be relatively consistent even when sample sizes vary (44). Therefore, we consider our sample sizes to be adequate for the questions we pose. A key advantage of our methods is that the results enable direct, robust comparisons between species. DNA extractions followed the standard protocol for animal tissues using the QIAGEN DNeasy Blood + Tissue Extraction Kit (45). Dual-indexed DNA libraries were prepared (46) and quantified using Qubit fluorimeter (Invitrogen, Inc., Carlsbad, CA). The libraries were pooled in sets of  $\sim$ eight and enriched for 5,060 UCE loci using the Tetrapods-UCE-5Kv1 kit from MYcroarray following version 1.5 of the UCE enrichment protocol and version 2.4 of the postenrichment amplification protocol (47). The resulting pools were combined and sequenced using a paired-end 150 protocol on an Illumina HiSeq 2500 using three lanes (Illumina, Inc., San Diego, CA; UCLA Neuroscience Genomics Core). Original sequence data have been deposited in the NCBI Sequence Read Archive (Supplemental Table S1; projects PRJNA741698, PRJNA741809, and PRJNA393740).

**Bioinformatics.** Raw and untrimmed FASTQ sequence data that contained low-quality bases were removed using Illumiprocessor (v.2.0.6 [48]). We built UCE reference sequences for each vector species by combining sequence read files (read1 plus singletons and read2) from two individuals (resulting in one read 1 and one read 2 file). We used the program Trinity (v.2.4.0 [49]) to assemble these reads *de novo* on the Galaxy platform (v.2.4 [50]), found and extracted UCE loci from this assembly using PHYLUCE (v.1.5.0 [51]) by matching the contigs to the probes set used, and then saved the resulting sequences as a reference FASTA. Single-nucleotide polymorphisms (SNPs) within the reference were coded using International Union of Pure and Applied Chemistry codes. Our bioinformatics pipeline focused on the package PHYLUCE, which calls many dependencies and identifies conserved orthologous loci that are then used as our reference set of UCE loci to call individual variants. Briefly, individual read1 (plus singletons) and read2 files were mapped to the taxon-specific reference and indexed using BWA-MEM (v.0.7.7 [52,53]) and SAMtools (v.0.1.19 [54]). Next, PICARD (v.1.106 [55]) was used to clean the alignments, add read group header information, and remove PCR and sequencing duplicates. SNPs were called for each individual against the reference sequence using Genome Analysis Toolkit module UnifiedGenotyper (GATK, v.3.3.0 [56]). GATK was also used to call and realign around indels, call and annotate SNPs, filter SNPs around indels, and then restrict data to high-quality SNPs. VCFtools (v.0.1.13 [57]) was used to filter the high-quality SNPs to create a complete matrix (all individuals represented at all loci) with a minimum genotype quality (Phred) score

of 10.0 (which equates to 90% confidence). The high-quality Variant Call Format (VCF) file was then thinned to 1 SNP/locus and made biallelic. We used BLASTn on National Center for Biotechnology Information (NCBI) to identify sex-linked loci (Z-linked) using our high-quality reference data of confidently surveyed loci, and resulting hits for Z-linked loci were then removed using a custom script (find\_chromy, v.1.2 [58]). Our thinned, biallelic VCF with Z-linked loci removed was used for our demographic analyses to estimate movement (i.e., gene flow).

**Demographic analyses to estimate gene flow.** Diffusion Approximations for Demographic Inference ( $\delta\text{a}\delta\text{i}$ , v.1.7.0 [59]) was used to estimate demographic parameters under best-fit models of pairwise divergence. Note that in population genomics models, "migration" equals gene flow and is not related to the seasonal migration of individuals. To find a best-fit model of demographic history, we tested eight divergence models (Supplemental Fig. S1): A) no divergence (neutral, populations never diverge), B) split with no migration (divergence without gene flow), C) split with migration (divergence with gene flow that is bidirectionally symmetric, 1 migration parameter), D) split with bidirectional migration (divergence with gene flow that is bidirectionally asymmetric, 2 migration parameters), E) split with exponential population growth, no migration, F) split with exponential population growth and migration, G) secondary contact with migration (1 migration parameter), and H) secondary contact with bidirectional migration (2 migration parameters).

For each pairwise comparison, we ran a series of optimization runs that consisted of running the model repeatedly to fine-tune model parameters. Following optimization, the best five log-likelihood scores from each set of subsequent runs were averaged to summarize that model. We used the Akaike information criterion (AIC) (60,61) to determine the best-fit model. Once the best-fit model was determined, it was run at least 15 times to obtain demographic parameter estimates, and we used these estimates from the best-fit model's top three runs to calculate biological estimates. Then the model was bootstrapped to provide a 95% confidence interval around each demographic parameter. To convert the best-fit model's demographic parameters to biologically relevant values, we determined generation time from the literature and estimated substitution rates (Supplemental Table S2) using BLASTn to compare each reference FASTA to a related avian genome with a fossil-calibrated node (62). These values were then used with the best-fit model demographic parameter estimates obtained from our analyses to provide estimates of ancestral population size ( $N_{\text{ref}}$ ), size of populations ( $nu1$ ,  $nu2$ ), time since split ( $T$ ), migration ( $M$ ; gene flow in individuals/generation, derived from the raw model output  $m$ ), migration from population 1 into population 2 (derived from  $m12$ ), migration from population 2 into population 1 (derived from  $m21$ ), and time of secondary contact ( $T_{\text{sc}}$ ) as appropriate (based on the best-fit model for each pairwise comparison).

**Scaling movement, harvest rates, and risk factors.** Estimates of gene flow from the demographic analysis in  $\delta\text{a}\delta\text{i}$  are based on long-term effective population sizes ( $N_e$ ), which is nearly always lower than census size in high-latitude birds (e.g., 40). These evolutionary average rates of gene flow are not scaled to census size, so they are very conservative, but they are directly comparable to each other. To consider these rates relative to census sizes, estimates of the latter were obtained from population estimates from the U.S. Fish and Wildlife Service (USFWS) (63) and from Wetlands International (64). The USFWS combines both greater and lesser scaup (*Aythya marila* and *Aythya affinis*) into one census estimate because the two species can be difficult to distinguish. To address this, we used the ratio of greater and lesser scaup obtained from the Bird Conservancy of the Rockies' global population estimates as part of their Partners in Flight, Avian Conservation Assessment Database (65). We applied this ratio to the USFWS (63) census estimate of "scaup" to obtain a census estimate for greater scaup alone. We used the proportion of gene flow ( $M$ , in individuals/generation) relative to  $N_e$

to scale our estimates of long-term gene flow up to approximately estimate contemporary gene flow by multiplying this proportion by census size: ( $M_{\text{Eurasia}}/N_e \text{ North America} \times \text{census size}$ ).

Subsistence harvest rates in Alaska were obtained from Naves and Otis (22) and Naves and Keating (24,66). Some subsistence species were not categorized with a species name, so the species categorized as “Teal” were used for green-winged teal (*Anas crecca crecca* and *A. c. carolinensis*), “Scaup” for greater scaup (*Aythya marila*), and “Small Shorebird” for common and Wilson’s snipe (*Gallinago gallinago* and *G. delicata*). We calculated the average annual harvest for each vector species across the years 2016, 2017, and 2018. To calculate a relative risk of potential exposure of Eurasian-origin AI virus to subsistence users, we estimated the number of individuals harvested of Eurasian origin given ( $M/N_e$ ) and annual harvest ( $M_{\text{Eurasia}}/N_e \times \text{annual harvest}$ ). Given high variation in AI infection rates (e.g., annual, seasonal, geographic), we did not add this as a variable but discuss our results in this context using available evidence for this region.

## RESULTS

**Estimated rates of gene flow.** The best-fit models for our demographic analyses in  $\delta a\delta i$  found gene flow present in all pairwise comparisons (Supplemental Table S3). In half of our comparisons (four species) the AIC analyses showed that some models fit the data similarly well, yielding a best-fit model and a runner-up model that was not statistically worse. These cases were in green-winged teal (*Anas crecca crecca* and *A. c. carolinensis*), greater scaup (*Aythya marila*), common eider (*Somateria mollissima*), and common and Wilson’s snipe (*Gallinago gallinago* and *G. delicata*). These runner-up models occurred between split-with-migration models and secondary-contact models (Supplemental Table S3). For demographic analyses we chose the best-fit model to be the one with the lowest AIC value, a  $\Delta AIC = 0$ , and a weighted AIC = 1 (Supplemental Tables S3, S4). The best-fit models were as follows: split with symmetric migration (Supplemental Fig. S1C) for northern pintail (*Anas acuta*), mallard (*Anas platyrhynchos*), and the greater scaup (*Aythya marila*); split with bidirectional (asymmetric) migration (Supplemental Fig. S1D) in common eider (*Somateria mollissima*), and the common and Wilson’s snipe (*Gallinago gallinago* and *G. delicata*) contrast; secondary contact with symmetric migration (Supplemental Fig. S1G) in long-tailed ducks (*Clangula hyemalis*); and secondary contact with bidirectional migration (Supplemental Fig. S1H) for green-winged teal (*Anas crecca crecca* and *A. c. carolinensis*) and the Eurasian and American wigeon (*Mareca penelope* and *M. americana*) contrast. From these best-fit models, the raw demographic parameter output (Supplemental Table S5) was used to calculate a biological estimate of the long-term average rates of gene flow (Supplemental Table S6).

Estimates for gene flow between Eurasian and North American vector species showed substantial levels of variation in movement (gene flow) between continental populations (Table 1, [67]). Values of individuals per generation varied across three orders of magnitude (Table 1). The dabbling ducks—northern pintail (*Anas acuta*), mallard (*Anas platyrhynchos*), Eurasian and American wigeon (*Mareca penelope* and *M. americana*), and green-winged teal (*Anas crecca crecca* and *A. c. carolinensis*)—showed the greatest magnitude of movements. Of these, northern pintail (*Anas acuta*) had the largest amount of movement (upwards of  $\sim 100$ – $300$  individuals/generation). The diving and sea ducks—long-tailed duck (*Clangula hyemalis*), greater scaup (*Aythya marila*), and common eider (*Somateria mollissima*)—showed a wide range in their levels of

movement. Of these ducks, the greatest magnitude of intercontinental movement occurred in long-tailed ducks (*Clangula hyemalis*;  $\sim 24$ – $87$  individuals/generation), while the lowest levels occurred in the common eider ( $\sim$ between one and two individuals/generation; Table 1). Our comparison of common and Wilson’s snipe (*Gallinago gallinago* and *G. delicata*) showed low levels of movement, with less than one individual/generation (Table 1).

Estimates of gene flow between Eurasian and North American populations as a proportion of  $N_e$  showed the proportion to be small across all species (Table 1). Of all these vector species, greater scaup (*Aythya marila*) had the highest proportion of movement into North America from Eurasia. The northern pintail (*Anas acuta*) had the highest proportion of movement into Eurasia from North America (Table 1).









**Relative risks of AI host species.** Gene flow as a proportion of  $N_e$  is conservative for contemporary populations, and scaling these values to census population sizes and annual harvest rates should result in more useful numbers for risk assessment. We did these calculations using the data from Table 1 to rank vector species in decreasing order of relative risk of intercontinental AI movement, both within the natural system (gene flow scaled to census size) and in the context of subsistence use (gene flow scaled to harvest rates; Table 2, [67]). The top three species in each context (though in slightly different order between each context) were greater scaup (*Aythya marila*), mallard (*Anas platyrhynchos*), and northern pintail (*Anas acuta*; Table 2). Other species, e.g., green-winged teal (*Anas crecca crecca* and *A. c. carolinensis*), Eurasian and American wigeons (*Mareca penelope* and *M. americana*), and long-tailed duck (*Clangula hyemalis*), were intermixed in their rankings. Finally, common eiders (*Somateria mollissima*) and common and Wilson’s snipe (*Gallinago gallinago* and *G. delicata*) were equivalently ranked in the two contexts (natural system and subsistence use) and had the lowest relative risk (Table 2).

The average annual harvest rates in Alaska (Table 1) show that three taxa, mallard (*Anas platyrhynchos*), northern pintail (*Anas acuta*), and Eurasian and American wigeons (*Mareca penelope* and *M. americana*), have the highest rates of harvest. When considering proportions of Eurasian-origin birds, two of these species, the mallard and northern pintail, are ranked numbers two and three (respectively) in relative risk for Asian-origin AI exposure (Table 2). Greater scaup (*Aythya marila*) has only a moderate level of harvest (Table 1), but when considering the estimated proportion of Asian-origin individuals, it had the highest risk of causing potential Asian-origin AI exposure to subsistence users (Table 2).

## DISCUSSION

Our study found that levels of intercontinental gene flow in waterbird AI vector species is highly variable. These results provide a solid quantitative framework for among-species contrasts in this AI risk assessment context. We show how population genomics methods can be applied to fill knowledge gaps to help understand the ecology of intercontinental pathogen movements, and to help subsistence users mitigate potential Eurasian-origin AI exposure. Among our sampled species, dabbling ducks overall had the highest rates of intercontinental movement as inferred from long-term average levels of gene flow. Variation in gene flow rates spanning orders of magnitude among AI vector species makes it clear that all do not pose similar risks of intercontinental virus movement (Table

Table 1. AI vector species of birds with estimated rates of gene flow between Eurasian and North American populations (individuals/generation, paired with the  $\pm 95\%$  confidence interval), movement between Eurasian and North American populations as a proportion of effective population size that is experiencing the influx (continent-based  $N_e$ ), average number of individuals harvested in Alaska (across years 2016, 2017, and 2018), and estimated census size in across North America. Illustrations were obtained and used with permission from Hines (67).

Vector Species		Gene flow into Eurasia from North America	Gene flow into North America from Eurasia	Gene flow into Eurasia as proportion of $N_e$	Gene flow into North America as proportion of $N_e$	Average Annual Harvest in Alaska	Estimated Census Size
<b>Northern Pintail</b> ( <i>Anas acuta</i> )		104.32 ( $\pm 0.14$ )	389.78 ( $\pm 0.53$ )	$9.93 \times 10^{-4}$	$7.11 \times 10^{-5}$	17,949	2,300,000
<b>Mallard</b> ( <i>Anas platyrhynchos</i> )		54.83 ( $\pm 0.31$ )	82.70 ( $\pm 0.47$ )	$1.62 \times 10^{-4}$	$7.10 \times 10^{-5}$	19,255	9,400,000
<b>Green-winged Teal</b> ( <i>Anas crecca crecca</i> – <i>A. c. carolinensis</i> )		23.31 ( $\pm 0.63$ )	18.35 ( $\pm 2.29$ )	$1.14 \times 10^{-5}$	$3.98 \times 10^{-5}$	5,224	3,200,000
<b>Eurasian and American Wigeons</b> ( <i>Mareca penelope</i> – <i>M. americana</i> )		24.24 ( $\pm 0.48$ )	3.17 ( $\pm 0.56$ )	$2.77 \times 10^{-5}$	$4.14 \times 10^{-5}$	10,724	2,800,000
<b>Long-tailed Duck</b> ( <i>Clangula hyemalis</i> )		23.84 ( $\pm 0.43$ )	86.89 ( $\pm 1.57$ )	$7.43 \times 10^{-4}$	$5.59 \times 10^{-5}$	4,537	1,000,000
<b>Greater Scaup</b> ( <i>Aythya marila</i> )		6.96 ( $\pm 0.22$ )	10.06 ( $\pm 0.32$ )	$6.60 \times 10^{-4}$	$3.16 \times 10^{-4}$	8,763	881,633
<b>Common Eider</b> ( <i>Somateria mollissima</i> )		2.14 ( $\pm 0.15$ )	0.86 ( $\pm 0.12$ )	$3.40 \times 10^{-5}$	$1.97 \times 10^{-5}$	8,534	1,297,000
<b>Common and Wilson's Snipe</b> ( <i>Gallinago gallinago</i> – <i>G. delicata</i> )		0.68 ( $\pm 0.04$ )	0.01 ( $\pm 0.05$ )	$1.28 \times 10^{-6}$	$1.18 \times 10^{-7}$	77	2,000,000

<sup>A</sup>Gene flow results from McLaughlin *et al.* (40).

















<sup>B</sup>Individuals categorized as “Teal” were used for green-winged teal comparison, “Scaup” for greater scaup, and “Small Shorebird” for common and Wilson’s snipe.

1), and we are able to provide relative risk rankings among the species studied (Table 2; Fig. 2, [67]). We note that the variation in movement among vector species could be due to variation in factors such as different life-history characteristics, patterns of dispersal, and behavioral tendencies. Assessments of population connectivity are particularly difficult for species that nest at high latitudes, as they often have large distributions across the annual cycle that span remote (uninhabited) landscapes, further reducing the detectability

of dispersal events and the ability to evaluate the magnitudes of movements occurring (68,69,70). Overall, our results showed that these vector species appear to vary by three orders of magnitude in the bird-to-bird natural system and by two orders of magnitude in the human-to-bird subsistence system (Tables 1, 2).

Contrasting rates of gene flow, census population sizes, and harvest should enable a more fine-tuned approach to AI risk mitigation, monitoring, and surveillance. However, this approach

Table 2. AI vector species of birds ranked in decreasing order of their relative risk of AI transmission to North American populations (left column) and to subsistence users (right column). Data are extrapolated from Table 1 gene flow estimates and reflect relative risk in terms of numbers of Eurasian individuals of each species projected to come into North America annually relative to that species' census size (left column) and the average annual subsistence harvest in Alaska (right column). Illustrations were obtained and used with permission from Hines (67).

Vector Species	Individuals of Eurasian origin given ( $M/N_e$ ) and census size	Vector species	Individuals of Eurasian origin given ( $M/N_e$ ) and annual harvest
<b>Mallard</b> <i>(Anas platyrhynchos)</i> 	667.42	<b>Greater Scaup</b> <i>(Aythya marila)</i> 	2.77
<b>Greater Scaup</b> <i>(Aythya marila)</i> 	278.71	<b>Mallard</b> <i>(Anas platyrhynchos)</i> 	1.37
<b>Northern Pintail</b> <i>(Anas acuta)</i> 	163.63	<b>Northern Pintail</b> <i>(Anas acuta)</i> 	1.28
<b>Green-winged Teal</b> <i>(Anas crecca crecca – A. c. carolinensis)</i> 	127.44	<b>Eurasian and American Wigeons</b> <i>(Mareca penelope – M. americana)</i> 	0.44
<b>Eurasian and American Wigeons</b> <i>(Mareca penelope – M. americana)</i> 	115.97	<b>Long-tailed Ducks</b> <i>(Clangula hyemalis)</i> 	0.25
<b>Long-tailed Ducks</b> <i>(Clangula hyemalis)</i> 	55.93	<b>Green-winged Teal</b> <i>(Anas crecca crecca – A. c. carolinensis)</i> 	0.21
<b>Common Eider</b> <i>(Somateria mollissima)</i> 	25.59	<b>Common Eider</b> <i>(Somateria mollissima)</i> 	0.17
<b>Common and Wilson's Snipe</b> <i>(Gallinago gallinago – G. delicata)</i> 	0.16	<b>Common and Wilson's Snipe</b> <i>(Gallinago gallinago – G. delicata)</i> 	0.02

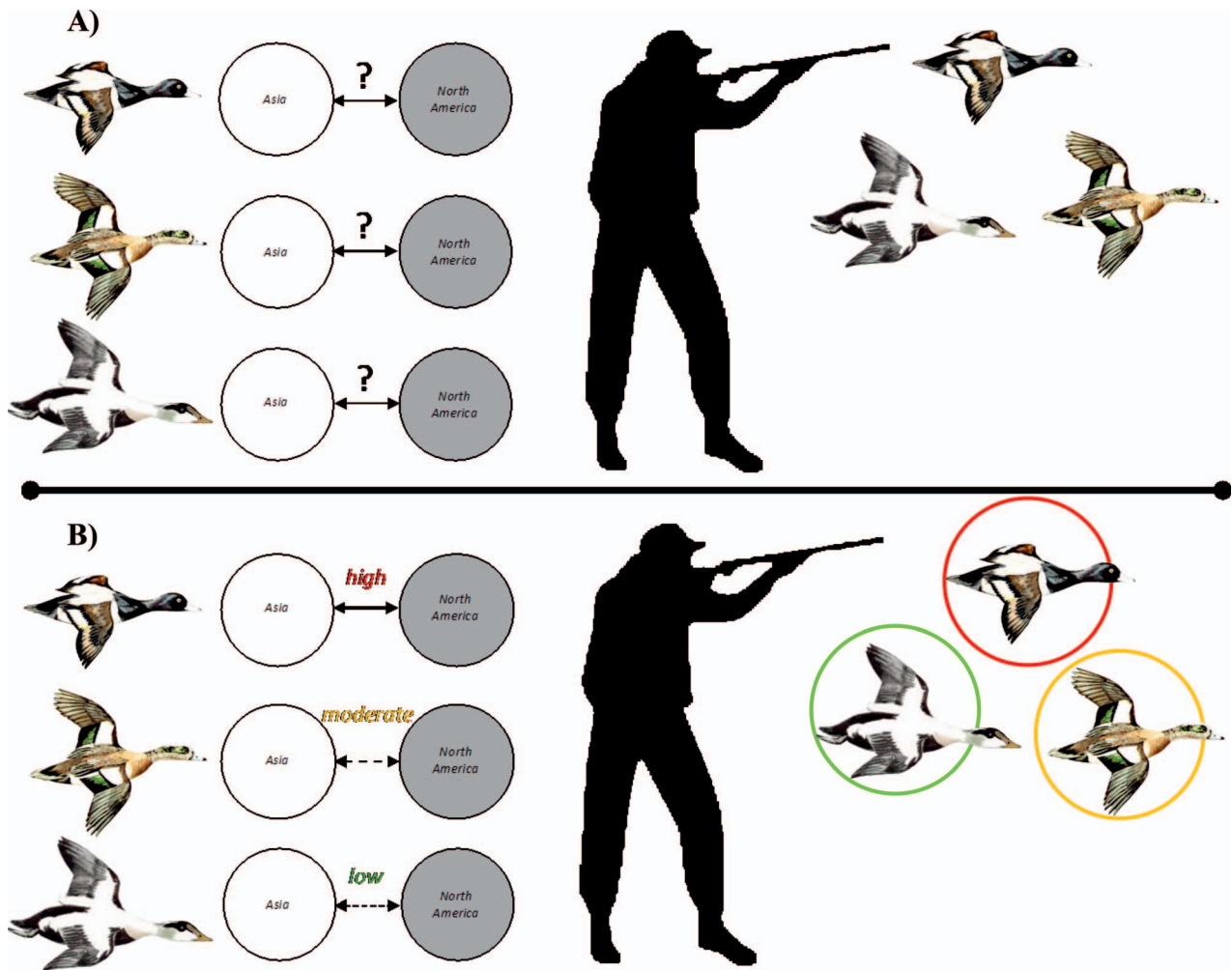


Fig. 2. How subsistence hunting could change to mitigate human exposure to Eurasian-origin avian influenza (AI). Species with high levels of intercontinental movement might be less desirable to harvest than species with low to moderate levels of intercontinental movement. **A)** Current understanding: unknown levels of intercontinental movement make it impossible to determine which species pose a high risk of possible Eurasian-origin AI exposure. **B)** This study shows intercontinental movements to be high in greater scaup (red), moderate in wigeons (yellow), and low in common eider (green) given the proportion of individuals of Eurasian origin given ( $M/N_e$ ) and annual harvest (Table 2). With this information, a subsistence hunter can choose to harvest species with lower intercontinental movements at higher rates to lower human risk of potential Eurasian-origin AI exposure. Illustrations obtained and used with permission from Hines (67).

does have limitations. First, we focused on the host movement system rather than on the viruses themselves. Infection rates are highly variable and are dependent on species, year, seasonality, and geographic location (1,15,71,72). Because infection rates are highly variable and are dependent on many factors, we did not incorporate them into our assessment of risk ranking at this time, although we provide some example data from Alaska surveillance to demonstrate how such next steps might proceed (Supplemental Table S7). In addition, HPAI strains often have different levels of pathogenicity and transmissibility between birds (73). Detailed understanding of these variables needs further development.

Secondly, we note that while our study design does not include all of the waterfowl species taken by subsistence hunters in this region, six of our eight study species are considered to be among the most commonly harvested species in Alaska (22,24,66). Estimates of AI prevalence in Alaska have shown that dabbling ducks (e.g., northern pintails) have the highest levels of AI infection (Supplemental Table S7) (13,15,28). Until these variables can be better estimated in this region, the basic attributes of the natural delivery system (e.g., gene

flow rates, census sizes) provide a useful initial baseline for relative risk assessment.

Gene flow is a measure (in evolutionary time) of contact between populations, and it is not equivalent to annual intercontinental movements of individuals. It does, however, provide an effective long-term metric, comparable among lineages, on which to base intercontinental AI movement risk assessments. Our estimates of gene flow are based on long-term  $N_e$ , and scaling up to census sizes is not straightforward. Long-term  $N_e$  values are generally smaller than modern census sizes, but among species the two are only loosely correlated (74). So while we have confidence that the relative rates of gene flow between populations are directly comparable among lineages across evolutionary time, converting those values to numbers of individuals given current census sizes (which themselves are only estimates; e.g., 75) represents an approximation. In addition, rates of gene flow can be affected by partial reproductive isolation between lineages, which would make them lower relative to actual movements. Furthermore, gene flow is an imperfect proxy for AI virus transmission because the latter can occur without host



reproduction and can easily occur across species, depending on varying levels of host resistance to AI viruses. Thus, while our analyses provide a robust contrast among codistributed lineages over the long term in an evolutionary context, annual variation is present and can only be approximated by our scaling to census sizes and harvest rates to estimate risk. Future work could involve pairing the results of this study with AI infection rates in each species for region, season, and year when such information becomes available (e.g., Supplemental Table S7).

Our study provides important details about the vector landscape through which AI viruses must navigate to move intercontinentally in this region. By quantifying the movements of vector species in terms of levels of gene flow and long-term  $N_e$ , we produce a robust metric enabling direct comparison among lineages that move intercontinentally in Beringia. By scaling these long-term movement rates to census sizes and harvest rates in Alaska (Table 1), we were able to estimate the relative risk that each species poses for Eurasian-origin AI viruses both in the natural virus delivery system and in the Alaska subsistence harvest (Table 2). We caution that variation in virus prevalence by species, season, year, and location will also strongly affect details of intercontinental transmission (e.g., Supplemental Table S7). But whether one is searching for viruses or trying to avoid them, having a map of the four-lane highways, two-lane highways, and dirt roads of the transport system will be useful. Our results are important in this context, giving subsistence hunters new information that can be used to choose to harvest species with a lower level of intercontinental movement and thus that pose a lower risk of Eurasian-origin AI exposure, rather than harvest species that might pose a higher risk (or to adopt appropriate personal protection, varying by species; Fig. 2). Likewise, prioritizing AI surveillance in species with high levels of intercontinental movement might be useful. Our baseline estimates of host-specific movements of AI vector species can be used to model, monitor, and mitigate AI virus movement in the Beringia region.

Supplemental data associated with this article can be found at <https://doi.org/10.1637/aviandiseases-D-21-00088.s1>.

## REFERENCES

1. Webster RG, Bean WJ, Gorman OT, Chambers TM, Kawaoka Y. Evolution and ecology of influenza A viruses. *Microbiol Rev.* 56:152–179; 1992.
2. Ferguson NM, Cummings DAT, Fraser C, Cajka JC, Cooley PC, Burke DS. Strategies for mitigating an influenza pandemic. *Nature* 442:448–452; 2006.
3. Cooper BS, Pitman RJ, Edmunds WJ, Gay NJ. Delaying the international spread of pandemic influenza. *PLoS Med.* 3:845–855; 2006.
4. Sellwood C, Asgari-Jirhandeh N, Salimee S. Bird flu: if or when? Planning for the next pandemic. *Postgrad Med J.* 83:445–450; 2007.
5. Pearce JM, Ramey AM, Flint PL, Koehler AV, Fleskes JP, Franson JC, Hall JS, Derksen DV, Ip HS. Avian influenza at both ends of a migratory flyway: characterizing viral genomic diversity to optimize surveillance plans for North America. *Evol Appl.* 2:457–468; 2009.
6. Ramey AM, Pearce JM, Flint PL, Ip HS, Derksen DV, Franson JC, Petrus MJ, Scotton BD, Sowl KM, Wege ML, *et al.* Intercontinental reassortment and genomic variation of low pathogenic avian influenza viruses isolated from northern pintails (*Anas acuta*) in Alaska: examining the evidence through space and time. *Virology* 401:179–189; 2010.
7. Ramey AM, Reeves AB, Donnelly T, Poulson RL, Stallknecht DE. Introduction of Eurasian-origin influenza A (H8N4) virus into North America by migratory birds. *Emerg Infect Dis.* 24:1950–1952; 2018.
8. Reeves AB, Pearce JM, Ramey AM, Ely CR, Schmutz JA, Flint PL, Derksen DV, Ip HS, Trust KA. Genomic analysis of avian influenza viruses from waterfowl in western Alaska, USA. *J Wildl Dis.* 49:600–610; 2013.
9. Reeves AB, Hall JS, Poulson RL, Donnelly T, Stallknecht DE, Ramey AM. Influenza A virus recovery, diversity, and intercontinental exchange: a multi-year assessment of wild bird sampling at Izembek National Wildlife Refuge, Alaska. *PLOS ONE* 13:e0195327; 2018.
10. Lee DH, Torchetti MK, Winker K, Ip HS, Song CS, Swayne DE. Intercontinental spread of Asian-origin H5N8 to North America through Beringia by migratory birds. *J Virol.* 89:6521–6524; 2015.
11. Horimoto T, Kawaoka Y. Pandemic threat posed by avian influenza A viruses. *Clin Microbiol Rev.* 14:129–149; 2001.
12. Krauss S, Webster RG. Avian influenza virus surveillance and wild birds: past and present. *Avian Dis.* 54:394–398. 2010.
13. Morin CW, Stoner-Duncan B, Winker K, Scotch M, Hess JJ, Meschke JS, Ebi KL, Rabinowitz PM. Avian influenza virus ecology and evolution through a climatic lens. *Environ Int.* 119:241–249; 2018.
14. Winker K, Gibson DD. The Asia-to-America influx of avian influenza wild bird hosts is large. *Avian Dis.* 54:477–482; 2010.
15. Winker K, McCracken KG, Gibson DD, Pruett CL, Meier R, Huettmann F, Wege M, Kulikova IV, Zhuravlev YN, Perdue ML, *et al.* Movements of birds and avian influenza from Asia into Alaska. *Emerg Infect Dis.* 13:547–552; 2007.
16. Flint PL, Ozaki K, Pearce JM, Guzzetti B, Higuchi H, Fleskes JP, Shimada T, Derksen DV. Breeding-season sympatry facilitates genetic exchange among allopatric wintering populations of northern pintails in Japan and California. *Condor* 111:591–598; 2009.
17. Hinshaw VS, Webster RG, Turner B. The perpetuation of orthomyxoviruses and paramyxoviruses in Canadian waterfowl. *Can J Microbiol.* 26:622–629; 1980.
18. Donis RO, Bean WJ, Kawaoka Y, Webster RG. Distinct lineages of influenza virus H4 hemagglutinin genes in different regions of the world. *Virology* 169:408–417; 1989.
19. Böning-Gaese K, González-Guzmán LI, Brown JH. Constraints on dispersal and the evolution of the avifauna of the Northern Hemisphere. *Evol Ecol.* 12:767–783; 1998.
20. Kilpatrick AM, Chmura AA, Gibbons DW, Fleischer RC, Marra PP, Daszak P. Predicting the global spread of H5N1 avian influenza. *Proc Natl Acad Sci U S A.* 103:9368–19373; 2006.
21. Rappole JH, Hubálek Z. Birds and influenza H5N1 virus movement to and within North America. *Emerg Infect Dis.* 12:1486–1492; 2006.
22. Naves LC, Otis D. *Alaska subsistence harvest of birds and eggs, 2016, Alaska Migratory Bird Co-Management Council.* Anchorage (AK): Alaska Department of Fish and Game Division of Subsistence Technical Paper No. 434; 2017.
23. U.S. Department of Agriculture. *2017 Census of agriculture.* Washington, DC: U.S. Department of Agriculture; 2019.
24. Naves LC, Keating JM. *Alaska subsistence harvest of birds and eggs, 2018, Alaska Migratory Bird Co-Management Council.* Anchorage (AK): Alaska Department of Fish and Game Division of Subsistence Technical Paper No. 464; 2020.
25. Lycett SJ, Bodewes R, Pohlmann A, Banks J, Banyai K, Boni MF, Bouwstra R, Breed AC, Brown IH, Chen H, *et al.* Role for migratory birds in the global spread of avian influenza H5N8. *Science* 354:213–217; 2016.
26. Ip HS, Flint PL, Franson JC, Dusek RJ, Derksen DV, Gill RE, Ely CR, Pearce JM, Lanctot RB, Matsuoka SM, *et al.* Prevalence of influenza A viruses in wild migratory birds in Alaska: patterns of variation in detection at a crossroads of intercontinental flyways. *Virology* 5:71; 2008.
27. Pearce JM, Reeves AB, Ramey AM, Hupp JW, Ip HS, Bertram M, Petrus MJ, Scotton BD, Trust KA, Meixell BW, *et al.* Interspecific exchange of avian influenza virus genes in Alaska: the influence of trans-hemispheric migratory tendency and breeding ground sympatry. *Mol Ecol.* 20:1015–1025; 2011.
28. Ramey AM, Reeves AB, Sonsthagen SA, TeSlaa JL, Nashold S, Donnelly T, Casler B, Hall JS. Dispersal of H9N2 influenza A viruses between East Asia and North America by wild birds. *Virology* 482:79–83; 2015.

29. Makarova NV, Kaverin NV, Krauss S, Senne D, Webster RG. Transmission of Eurasian avian H2 influenza virus to shorebirds in North America. *J Gen Virol*. 80:3167–3171; 1999.
30. Liu JH, Okazaki K, Bai GR, Shi WM, Mweene A, Kida H. Interregional transmission of the internal protein genes of H2 influenza virus in migratory ducks from North America to Eurasia. *Virus Genes*. 29:81–86; 2004.
31. Gill JS, Webby R, Gilchrist MJR, Gray GC. Avian influenza among waterfowl hunters and wildlife professionals. *Emerg Infect Dis*. 12:1284–1286; 2006.
32. Dishman H, Stallknecht D, Cole D. Duck hunters' perceptions of risk for avian influenza, Georgia, USA. *Emerg Infect Dis*. 16:1279–1281; 2010.
33. Brown JD, Stallknecht DE, Valeika S, Swayne DE. Susceptibility of wood ducks to H5N1 highly pathogenic avian influenza virus. *J Wildl Dis*. 43:660–667; 2007.
34. Siembieda J, Johnson CK, Boyce WM, Sandrock C, Cardona C. Risk for avian influenza virus exposure at human-wildlife interface. *Emerg Infect Dis*. 14:1151–1153; 2008.
35. Gilsdorf A, Boxall N, Gasimov V, Agayev I, Mammadzade F, Ursu P, Gasimov E, Brown C, Mardel S, Jankovic D, et al. Two clusters of human infection with influenza A/H5N1 virus in the Republic of Azerbaijan, February–March 2006. *Euro Surveill*. 11:122–126; 2006.
36. Yamamoto Y, Nakamura K, Yamada M, Mase M. Persistence of avian influenza virus (H5N1) in feathers detached from bodies of infected domestic ducks. *Appl Environ Microbiol*. 76:5496–5499; 2010.
37. Dórea FC, Cole DJ, Stallknecht DE. Quantitative exposure assessment of waterfowl hunters to avian influenza viruses. *Epidemiol Infect*. 141:1039–1049; 2013.
38. Humphries EM, Winker K. Discord reigns among nuclear, mitochondrial and phenotypic estimates of divergence in nine lineages of trans-Beringian birds: discord among divergence estimates. *Mol Ecol*. 20:573–583; 2011.
39. Peters JL, McCracken KG, Pruett CL, Rohwer S, Drovetski SV, Zhuravlev YN, Kulikova I, Gibson DD, Winker K. A parapatric propensity for breeding precludes the completion of speciation in common teal (*Anas crecca*, sensu lato). *Mol Ecol*. 21:4563–4577; 2012.
40. McLaughlin JF, Faircloth BC, Glenn TC, Winker K. Divergence, gene flow, and speciation in eight lineages of trans-Beringian birds. *Mol Ecol*. 29:3526–3542; 2020.
41. Faircloth BC, McCormack JE, Crawford NG, Harvey MG, Brumfield RT, Glenn TC. Ultraconserved elements anchor thousands of genetic markers spanning multiple evolutionary timescales. *Syst Biol*. 61:717–726; 2012.
42. Felsenstein J. Accuracy of coalescent likelihood estimates: do we need more sites, more sequences, or more loci? *Mol Biol Evol*. 23:691–700; 2005.
43. Nazareno AG, Bemmels JB, Dick CW, Lohmann LG. Minimum sample sizes for population genomics: an empirical study from an Amazonian plant species. *Mol Ecol Resour*. 17:1136–1147; 2017.
44. McLaughlin JF, Winker K. An empirical examination of sample size effects on population demographic estimates in birds using single nucleotide polymorphism (SNP) data. *PeerJ* 8:e9939; 2020.
45. QIAGEN. *DNeasy blood & tissue handbook*. Germantown (MD): QIAGEN; 2006.
46. Glenn TC, Nilsen Kieran TJ, Sanders JG, Bayona-Vasquez NJ, Finger Jr. JW Pierson TW, Bentley KE, Hoffberg SL, Louha S, et al. Adapterama I: Universal stubs and primers for 384 unique dual-indexed or 147,456 combinatorially-indexed Illumina libraries (iTru & iNext). *PeerJ* 7:e7755; 2019.
47. Ultraconserved Elements (UCE). *Tetrapod Probe Set: Tetrapods-UCE-5Kv1*. [modified: 2019, Jan 4; accessed: 2022, March 8]. <http://ultraconserved.org/>.
48. Faircloth BC. Illumiprocessor: a trimmomatic wrapper for parallel adapter and quality trimming. 2013. [modified: 2021, Jan 29; accessed 2022, March 8]. <http://dx.doi.org/10.6079/J9ILL>
49. Grabherr MG, Haas BJ, Yassour M, Levin JZ, Thompson DA, Amit I, Adiconis X, Fan L, Raychowdhury R, Zeng Q, et al. Full-length transcriptome assembly from RNA-Seq data without a reference genome. *Nat Biotechnol*. 29:644–652; 2011.
50. Afgan E, Baker D, van den Beek M, Blankenberg D, Bouvier D, Čech M, Chilton J, Clements D, Craor N, Eberhard C, et al. The Galaxy platform for accessible, reproducible and collaborative biomedical analyses. *Nucleic Acids Res*. 44:3–10; 2016.
51. Faircloth BC. PHYLUCS is a software package for the analysis of conserved genomic loci. *Bioinformatics* 32:786–788; 2016.
52. Li H, Durbin R. Fast and accurate short read alignment with Burrows-Wheeler transform. *Bioinformatics* 25:1754–1760; 2009.
53. Li H. Aligning sequence reads, clone sequences and assembly contigs with BWA-MEM. *arXiv:1303.3997v1*; 2013.
54. Li H, Handsaker B, Wysoker A, Fennell T, Ruan J, Homer N, Marth G, Abecasis G, Durbin R. the sequence alignment/map format and SAMtools. *Bioinformatics* 25:2078–2079; 2009.
55. Broad Institute. *Picard toolkit*. Cambridge (MA): Broad Institute. <http://broadinstitute.github.io/picard/>; 2019.
56. McKenna A, Hanna M, Banks E, Sivachenko A, Cibulskis K, Kernytsky A, Garimella K, Altshuler D, Gabriel S, Daly M, et al. The Genome Analysis Toolkit: a mapreduce framework for analyzing next-generation DNA sequencing data. *Genome Res*. 20:1297–1303; 2010.
57. Danecek P, Auton A, Abecasis G, Albers CA, Banks E, DePristo MA, Handsaker RE, Lunter G, Marth GT, Sherry ST, et al. The variant call format and VCFtools. *Bioinformatics* 27:2156–2158; 2011.
58. Beringia Scripts. *Scripts written for Beringia population genomics project bioinformatics pipeline*, version 1.2. [https://github.com/jfmclaughlin92/beringia\\_scripts/](https://github.com/jfmclaughlin92/beringia_scripts/)
59. Gutenkunst RN, Hernandez RD, Williamson SH, Bustamante CD. Inferring the joint demographic history of multiple populations from multidimensional SNP frequency data. *PLoS Genet*. 5:e1000695; 2009.
60. Akaike H. A new look at the statistical model identification. *IEEE Trans Automatic Control* 19:716–723; 1974.
61. Burnham KP, Anderson DR. Multimodel inference: understanding AIC and BIC in model selection. *Sociolog Methods Res*. 33:261–304; 2004.
62. Claramunt S, Cracraft J. A new time tree reveals Earth history's imprint on the evolution of modern birds. *Sci Adv*. 1:e1501005; 2015.
63. U.S. Fish and Wildlife Service. *Waterfowl population status, 2019*. Washington (DC): U.S. Department of the Interior; 2019.
64. Wetlands International. 2021. *Waterbird population estimates*. [modified 2021 May 30; accessed 2021 May 30] <http://wpe.wetlands.org>.
65. Partners in Flight. *Avian conservation assessment database and population estimates handbook (ACAD); version 3.1*. [modified 2020 Sept 4; accessed 2021 May 30]. <https://pif.birdconservancy.org/>.
66. Naves LC, Keating JM. Alaska subsistence harvest of birds and eggs, 2017, Alaska Migratory Bird Co-Management Council. Anchorage (AK): Alaska Department of Fish and Game Division of Subsistence Technical Paper No. 443; 2018.
67. Hines B. *Ducks at a distance: a waterfowl identification guide*. Albuquerque (NM): U.S. Department of the Interior, Fish and Wildlife Service. 1963.
68. Sonsthagen SA, Talbot SL, Scribner KT, McCracken KG. Multi-locus phylogeography and population structure of common eiders breeding in North America and Scandinavia. *J Biogeogr*. 38:1368–1380; 2011.
69. Talbot SL, Sonsthagen SA, Pearce JM, Scribner KT. Phylogenetics, phylogeography and population genetics of North American sea ducks (tribe: Mergini). *Ecol Conserv N Am Sea Ducks; Stud Avian Biol*. 46:29–62; 2015.
70. Sonsthagen SA, Wilson RE, Lavretsky P, Talbot SL. Coast to coast: high genomic connectivity in North American scoters. *Ecol Evol*. 9:7246–7261; 2019.
71. Dushoff J, Plotkin JB, Levin SA, Earn DJD. Dynamical resonance can account for seasonality of influenza epidemics. *Proc Natl Acad Sci*. 101:16915–16916; 2004.
72. Altizer S, Dobson A, Hosseini P, Hudson P, Pascual M, Rohani P. Seasonality and the dynamics of infectious diseases. *Ecol Lett*. 9:467–484; 2006.
73. Shi W, Gao GF. Emerging H5N8 avian influenza viruses. *Science* 372:784–86; 2021.

74. Roman J. Whales before whaling in the North Atlantic. *Science* 301:508–510; 2003.

75. Barclay JS. 2012. *Status of greater scaup in North America*. Storrs (CT): University of Connecticut. [modified 2012 Feb 14; accessed 2021 May 30]. <https://globally-threatened-bird-forums.birdlife.org/wp-content/uploads/2011/11/Greater-ScaupStatus-14Feb12-J-Barclay.doc>

#### ACKNOWLEDGMENTS

We thank the University of Alaska Museum and the University of Washington Burke Museum for loans of tissue specimens, Troy Kieran and members of the EHS DNA lab for processing samples, and the specimen collectors who made it possible to do this research. We also thank the Kessel Fund for Northern Ornithology and the Friends of Ornithology for financial support, and Brant Faircloth for

his input early in the project. This project was funded in part by the National Science Foundation (DEB-1242267-1242241-1242260), by an Institutional Development Award (IDeA) from the National Institute of General Medical Sciences of the National Institutes of Health under grant number 2P20GM103395, and by the National Institute of General Medical Sciences of the National Institutes of Health under award number RL5GM118990. Naoki Takebayashi, Devin Drown, and two anonymous reviewers provided helpful comments and feedback on earlier drafts of the manuscript. The study was conceived by Kevin Winker, Travis Glenn, and Brant Faircloth. The data were generated by Travis Glenn's lab and Brant Faircloth. The data were analyzed by Fern Spaulding. The first draft was written by Fern Spaulding. All authors contributed to the final version.